ELSEVIER

Vibrational Spectroscopy 26 (2001) 113–131

VIBRATIONAL SPECTROSCOPY

www.elsevier.com/locate/vibspec

A combined matrix-isolation infrared spectroscopy and MO study of 1-amino-2-propanol

Constança Cacela[a], Rui Fausto[b,*], Maria Leonor Duarte[a]

[a]*Departamento de Química e Bioquímica, CECUL, Faculdade de Ciências, Universidade de Lisboa, 1749-016 Lisboa, Portugal*
[b]*Departamento de Química (CQC), Universidade de Coimbra, 3004-535 Coimbra, Portugal*

Received 23 January 2001; received in revised form 28 March 2001; accepted 18 April 2001

Abstract

Vibrational spectra of 1-amino-2-propanol (**1AP**) isolated in argon and krypton matrices at 14 K and of the pure liquid at room temperature were recorded and interpreted on the basis of ab initio MO calculations undertaken at the HF-SCF and MP2 levels of theory. For the first time, five different conformational states of monomeric **1AP** could be experimentally observed and their vibrational signatures obtained. The observed conformers were found to correlate well with the most stable forms predicted by the MP2 calculations, the first and second lowest energy forms corresponding to conformers which exhibit a considerably strong intramolecular OH···N hydrogen bond (gG′g and g′Gg′), while the less abundant forms observed in the matrices (tG′t, g′G′t and tG′g′) are characterized by having a relatively weak intramolecular NH···O bond. These results were reinforced by infrared solution studies of the compound in tetrachloroethylene. The experimental data obtained for the pure liquid, where OH···N intermolecular hydrogen bonding dominates, indicate that the preferred conformation of the monomeric unit within the aggregates is similar to conformer tG′t.

Keywords: 1-Amino-2-propanol; Intra- and intermolecular hydrogen bonding; Infrared and Raman spectra; Matrix-isolation; HF-SCF and MP2 6-31G* ab initio calculations

1. Introduction

Aminoalcohols show appropriate physical properties for their use as vitrifying agents, with potential application in long-term cryopreservation of biological tissues and organs [1,2]. The vitrifying ability of these compounds, i.e. the property of avoiding ice formation upon lowering the temperature to sub-zero temperatures when they are added to water in a given proportion, has been suggested to be controlled, at least in part, by different types of inter- and intramolecular hydrogen bonds in which aminoalcohols can be involved [2].

The study of the monomeric species of these kinds of molecules is then essential to obtain the relevant information on their structures and conformational behavior and to characterize the main intramolecular interactions that are operating in these forms. Once the monomeric species are well characterized, the acquired information could then be used as a basis to interpret the experimental data obtained in condensed phases and to evaluate the dominant intermolecular interactions that are operating under these conditions.

With this in view, we have recently started a systematic study of a series of simple aminoalcohols by matrix-isolation infrared spectroscopy and molecular

* Corresponding author. Tel.: +351-2-39-852080; fax: +351-2-39-827703.
E-mail address: rfausto@ci.uc.pt (R. Fausto).

0924-2031/01/$ – see front matter
PII: S0924-2031(01)00112-6

orbital calculations, complemented by conventional liquid phase infrared and Raman spectroscopy. The molecules already studied include 2-aminoethanol (**2AE**) [3], 3-amino-1-propanol (**3AP**) [4] and 2-amino-1-propanol (**2AP**) [5], for which we were able to identify the most stable conformers and characterize the most important intramolecular interactions that are responsible for their relative stability. It could be well established that, for the isolated molecules, OH···N and NH···O intramolecular hydrogen bonding may occur, the former being considerably stronger than the latter and being present in the most stable conformers of all molecules studied [3–5]. A plot of *ν*OH versus the OH···N distance in the previously studied molecules was found to obey to a straight line correlation and demonstrated a progressive strengthening of the intramolecular OH···N hydrogen bond in the most stable conformer of each molecule in the order **2AE** < **2AP** < **3AP** [5]. The better ability of **3AP** to take part in hydrogen bonding could be ascribed to the greater conformational flexibility of this molecule which leads to a more favorable interaction geometry [4,5]. On the other hand, the presence of the extra methyl group attached to the carbon atom bearing the amino group in **2AP** was pointed out as the main cause justifying the stronger OH···N intramolecular hydrogen bond in this compound when compared with **2AE**, since it leads to an increased basicity of the amino group [5].

In the liquid phase, OH···N intermolecular hydrogen bonding becomes the dominant interaction and the NH···O intramolecular hydrogen bonding was found to play a prominent role in stabilizing the conformations assumed by the monomeric units within the aggregates [3–5]. In agreement with the strongest intramolecular OH···N hydrogen bond present in the conformational ground state of **3AP**, which reduces its tendency to aggregate, the spectroscopic data obtained for this molecule clearly show that monomers assuming this conformation are also present in detectable amounts in the pure liquid [4], while for **2AE** and **2AP**, where the intramolecular OH···N hydrogen bonding is considerably weaker than in **3AP**, no experimental evidence could be found for the presence of monomeric species in the pure liquids [3,5].

In this paper, we present results obtained for 1-amino-2-propanol (**1AP**), following a similar approach to that used in our previous studies on **1AE**, **2AP** and **3AP** [3–5]. This compound was studied previously by microwave spectroscopy [6], the experimental results indicating that the most abundant conformer in the gaseous phase, at room temperature, corresponds to a conformer with an OH···N intramolecular hydrogen bond where the amino and methyl groups are anti to each other. No other conformers could be observed by microwave spectroscopy and a lower limit of ca. 4 kJ mol^{-1} was estimated for the excess energy of other conformational states relatively to the most stable conformer [6]. To the best of our knowledge no further studies were reported on this molecule.

2. Experimental

The D isomer of **1AP**, obtained commercially (Aldrich, spectroscopic grade, purity >98%), was used without any additional purification. The sample was handled in a glove box to avoid moisture from air. To undertake the matrix-isolation infrared studies, the sample was premixed with Ar (99.999% purity) or Kr (99.998%) under reduced pressure. The gas mixtures (matrix:solute = 1000) thus formed were then sprayed onto the cold KBr window at 14 K. The gas flux was controlled with two Swagelok valves (models BMG and BMRG), which make the connection to an APD cryogenics DMX closed cycle helium refrigeration system whose principal component is a DE-202 Displex expander. The refrigeration system is supported by an APD cryogenics helium compressor (model HC-2D-1). For the conventional IR spectra a specially designed demountable transmission variable temperature cell with KBr windows, linked to a T48 (Red Lion Controls) temperature controller was used. The IR spectra were obtained using a Mattson (infinity series) or a Bomem (MB104) Fourier transformer spectrometer equipped with a deuterated triglycine sulfate (DTGS) detector and Ge/KBr or Zn/Se optics. Data collection was performed with 1 cm^{-1} spectral resolution. Solution studies were undertaken at room temperature using $Cl_2C{=}CCl_2$ (Merck, purity >99%) as solvent and covering a concentration range from 50×10^{-3} to 150×10^{-3} M.

Raman spectrum was obtained using a Spex 1403 double monochromator spectrometer (focal length

0.85 m, aperture *f*/7.8) equipped with holographic gratings with 1800 groove/mm (reference 1800-1SHD). The 514.5 nm Ar^+ laser, adjusted to provide 220 mW power at the sample, was used as excitation radiation. Detection was effected using a thermoelectrically cooled Hamamatsu R928 photomultiplier. The spectrum was recorded using increments of 1 cm^{-1} and integration times of 1 s.

Band intensities were obtained from the area of the observed peaks, subjected to previous deconvolution by using the peak-fitting module of ORIGIN 4.0 [7]. A simulation of the calculated HF 6-31G* spectrum of isolated **1AP** was performed by Gaussian synthesis, from the scaled ab initio frequencies and intensities, using the SYNSPEC program [8].

The ab initio molecular orbital calculations were performed using the 6-31G* basis set [9] with the GAUSSIAN92/DFT program package [10] running on a DEC ALPHA 7000 computer. Molecular geometries were fully optimized by the force gradient method using Berny's algorithm [11] and the standard convergence criteria for the geometry optimization both at the Hartree–Fock and MP2 levels of theory. The HF 6-31G* ab initio calculated vibrational spectra were then used to help interpretation of the spectroscopic results, the calculated wave numbers being scaled down in order to fit to the experimental values by using a single scale factor (0.89 [12]). Normal coordinate analysis was undertaken using the programs TRANSFORMER, BUILD-G and VIBRAT [13] which are interfaced with GAUSSIAN92.

3. Results and discussion

Internal rotations about C–N, C1–C2, and C–O bonds in **1AP** can give rise to conformational isomerism. In the stable conformations, the values of the dihedral angles associated with these internal rotations are expected to be, in all cases, close to 60, −60 and 180°. This makes the total number of candidate structures to be a minimum in the potential energy surface of **1AP** equal to 27. To name the conformers, we used three letters, the first referring to the configuration around the C–N bond, the second and third to the configuration around the C1–C2 and C–O bonds, respectively; the letters g/G, g′/G′ and t/T indicate dihedral angles close to 60, −60 and 180°, respectively (lp-N–C1–C2 (lp = lone pair), N–C–C–O and C1–C2–O–H dihedral angles were taken as reference angles). Lower case letters apply to lp-N–C1–C2 and C1–C2–O–H axes; capital letters to N–C–C–O axis. Since C2 is a chiral center, **1AP** exists in two enantiomeric forms (D and L), but these should have similar intramolecular interactions and give rise to identical vibrational spectra.

3.1. Molecular structures and energies

In this study, the 27 structures having the appropriate combination of values of the lp-N–C1–C2, N–C–C–O and C1–C2–O–H dihedral angles (lp = lone pair) were given as input to the minimizing program. After minimization, all but two of these structures converged to the corresponding local minima in the HF potential energy surface of **1AP**. The two exceptions are the gG′g′ and g′Gg initial conformations, where considerably strong steric interactions between the hydroxyl group and either the methyl or amino groups were expected to occur. These structures converged to the most stable gG′g and g′Gg′ forms, respectively, from which they may easily be obtained by internal rotation around the C2–O axis. On the other hand, at the MP2 level of theory only 23 stable structures were found. In this case, in addition to gG′g′ and g′Gg, minimization of the g′G′g and gGg′ initial conformations also converged to the most stable gG′g and g′Gg′ conformers, respectively, from which they differ by internal rotation about the C–N bond. The relative energies of all calculated minima are shown in Table 1. The five most stable conformers, as predicted by the higher-level MP2 calculations, are depicted in Fig. 1 and their calculated geometries, relative energies and predicted populations at 298 K (assuming a Boltzmann distribution) are presented in Table 2.[1]

Considering the sum of van der Waals radii of (H + N) = 270 and (H + O) = 260 pm [14], conformers gG′g and g′Gg′, with $d(\mathrm{OH}\cdots\mathrm{N}) < 270$ pm, and conformer tG′t, g′G′t and tG′g′, with $d(\mathrm{NH}\cdots\mathrm{O}) < 260$ pm, are considered to be stabilized by an $\mathrm{OH}\cdots\mathrm{N}$ or $\mathrm{NH}\cdots\mathrm{O}$ intramolecular hydrogen bond, respectively. In the two most stable conformers (gG′g, g′Gg′) the $d(\mathrm{OH}\cdots\mathrm{N})$ distance is

[1] Complete structural data for the higher energy local minima may be obtained from the corresponding author upon request.

Table 1
Zero point vibrational energy corrected relative energies, at the MP2/6-31G* and HF/6-31G* levels of theory, for the different conformations of 1-amino-2-propanol

Conformer	ΔE (kJ/mol)	
	MP2	HF
gG′g	0.00	0.00
g′Gg′	4.04	4.79
g′G′g	[a]	6.71
tG′t	10.23	7.98
g′G′t	10.63	7.44
tG′g′	10.75	9.72
gGg′	[b]	9.73
gGt	11.58	9.68
tGg	12.24	11.84
tGt	12.61	11.33
g′G′g′	12.71	10.57
gGg	13.89	12.34
tG′g	14.84	12.81
g′Tt	15.97	11.46
g′Tg′	16.99	13.15
tTg	17.00	14.31
g′Tg	17.26	13.13
gTt	17.68	13.02
gTg	17.69	13.44
tGg′	17.86	16.89
tTg′	18.28	15.69
tTt	18.29	13.98
gTg′	18.68	14.88
g′Gt	27.04	24.28
gG′t	27.45	22.56

[a] g′G′g converged to the most stable form gG′g at the MP2 6-31G* level.
[b] gGg′ converged to the most stable form g′Gg′ at the MP2 6-31G* level.

much smaller than the sum of the van der Waals radii of (H + N) (see Table 2) and the hydrogen bonding can be expected to be strong, being the most important intramolecular stabilizing factor acting in these two conformers and justifying their considerably lower energy when compared with the remaining conformers. In consonance with the microwave estimations [6], the second most stable form (g′Gg′) has an energy ca. 4 kJ mol^{-1} above the conformational ground state (gG′g). On the other hand, the additional conformer located in the MP2 potential energy surface exhibiting a d(OH···N) distance smaller than the sum of the van der Waals radii of (H + N) (conformer tG′g), has a considerably higher energy than the two lowest energy conformers: $\Delta E^{MP2}_{tG'g-gG'g} = 14.84$ kJ mol^{-1}. This result correlates well with the much longer d(OH···N) distance calculated for the higher energy tG′g conformer (265.1 pm), when compared with that distance in the gG′g and g′Gg′ forms, which is a clear indication that in this form the OH···N bond is of considerably weaker importance.

The relative energies of gG′g and g′Gg′ can also be correlated with the strength of the OH···N bond in these forms. In fact, d(OH···N) is shorter in gG′g than in g′Gg′ (212.4 pm versus 214.8 pm), showing that the hydrogen bond is stronger in the most stable gG′g conformer. In form g′Gg′, the CH_3 group is positioned *gauche* in relation to the amino group while in form gG′g these groups are *trans* to each other. The *gauche* arrangement in g′Gg′ results in a closer distance between the methyl and amino groups, leading to a small steric repulsion between these moieties the distance between the two closest hydrogen atoms of these groups is predicted by the MP2 calculations to be 238.4 pm, i.e. shorter than the sum of the (H + H) van der Waals radii (240.0 pm). In order to minimize this steric repulsion, changes in the dihedral angles must occur, leading to the observed longer d(OH···N) distance and to a weaker hydrogen bond interaction.

Using the criteria based on the van der Waals radii, described above, there are several stable conformations of **1AP** predicted by the calculations to have an NH···O intramolecular hydrogen bond. As predicted by the MP2 calculations, besides conformers tG′t, g′G′t and tG′g′ (which correspond to the third, fourth and fifth most stable conformers), five other conformers exhibit an NH···O bond. These conformers correspond to the 6th to the 10th conformers in the energy scale (see Table 1). Despite the fact that NH···O hydrogen bond is in all probability the main factor responsible for the stabilization of all these eight conformers, it is however clear, from the calculated d(NH···O) distances as well as from their relative energies, that this interaction is, in all cases, relatively weak.

All the above results follow the same trend previously found for **2AP**, where the OH···N hydrogen bonding was also found to be considerably more important than the NH···O interaction in stabilizing the different conformers [5]. In addition, the most important repulsive (destabilizing) intramolecular interactions present in the whole set of conformers

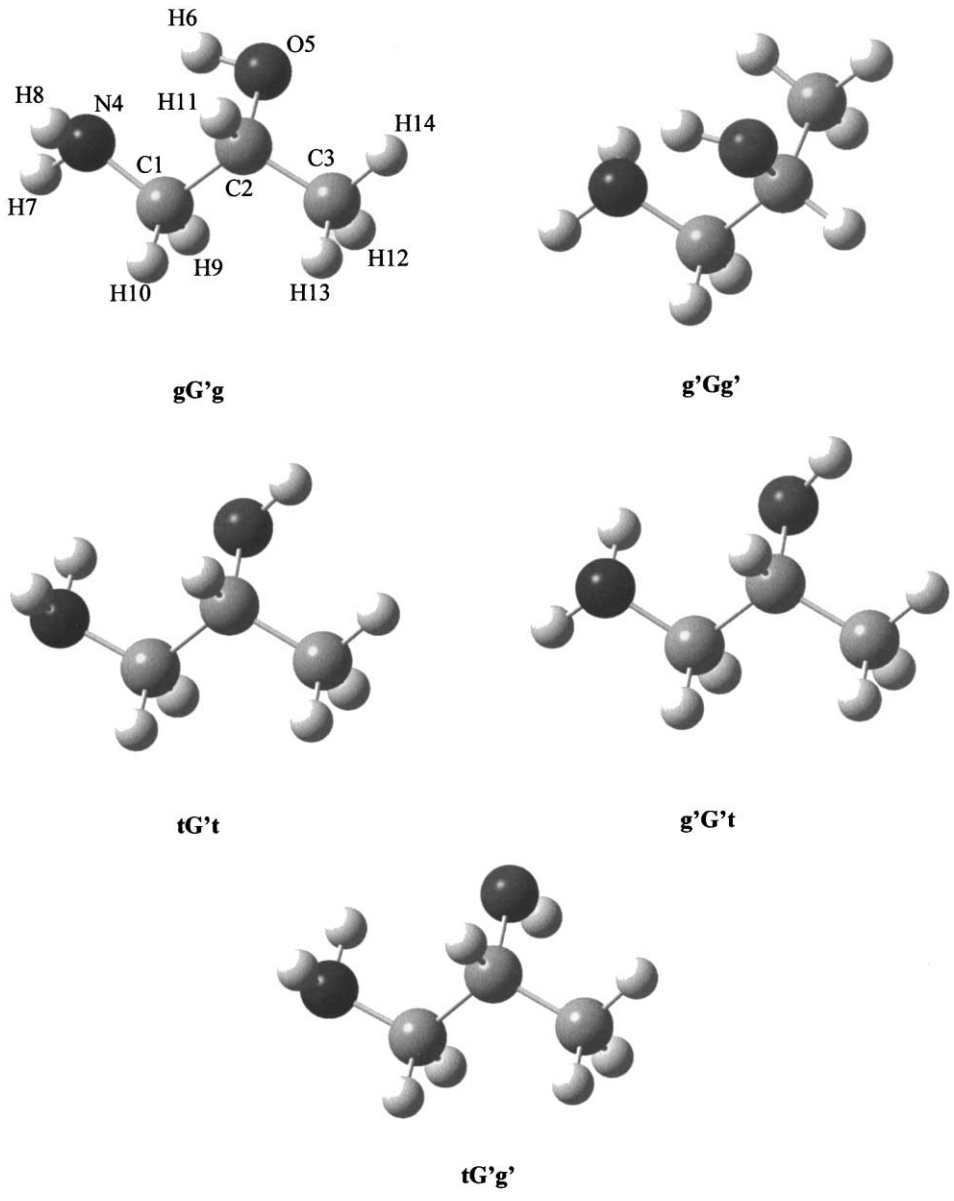

Fig. 1. The most stable conformers of 1-amino-2-propanol and atom numbering scheme.

of **1AP** are also similar to those observed for **2AP** [5]. So, the energies of the highest energy conformers (e.g. gG′t and g′Gt) are mainly determined by the presence of the strongly repulsive interaction between the lone electron pairs of the oxygen and nitrogen atoms (see Table 1), this interaction being by far the strongest repulsive interaction that can operate in the studied molecule, while the less important $OH\cdots H_3C$, $OH\cdots HC$ or $OH\cdots HN$ repulsive interactions are the main factors contributing to the relatively high energy of the remaining high energy conformers, the first one being the most relevant in energetic terms.

It is also interesting to compare the results obtained at the two levels of theory used. With the notable exception of the second most stable conformer, g′Gg′, all energies relative to the most stable form are

predicted to be larger by the MP2 than by the HF calculations. This result was also found previously for **2AP** [5] and means essentially that the higher-level MP2 calculations lead to an additional stabilization of the two most stable conformers. Since the most important stabilizing factor in these two forms is the presence of a relatively strong OH···N intramolecular hydrogen bond, this result clearly shows the

Table 2
Some calculated relevant structural and energetic data for the most stable forms of 1-amino-2-propanol[a]

	gG′g		g′Gg′	tG′t	g′G′t	tG′g′
	Ref [6][b]	MP2	MP2	MP2	MP2	MP2
ΔE		–	4.04	10.23	10.63	10.75
ΔE^{c}		–	4.79	7.98	7.44	9.72
p^{d}		78.0 (1.00)	15.3 (0.20)	1.3 (0.02)	1.1 (0.01)	1.0 (0.01)
$p^{c,d}$		69.0 (1.00)	10.0 (0.14)	2.8 (0.04)	3.4 (0.05)	1.4 (0.02)
Bond length						
C1–C2	152.6	152.5	152.9	152.4	151.6	152.8
C2–C3	152.6	151.5	152.5	152.0	152.0	152.0
C–N	147.5	147.0	147.2	146.1	146.3	146.2
C–O	139.6	142.1	142.4	143.5	143.8	143.7
O–H	113.9	98.0	98.0	97.2	97.2	97.5
N–H7	101.7	101.8	101.8	102.0	101.9	102.0
N–H8	101.7	101.9	101.7	101.9	101.9	102.0
C–H9	109.3	110.1	109.4	109.6	109.6	109.6
C–H10	109.3	109.5	110.0	109.6	110.3	109.9
C–H11	109.3	110.5	109.6	110.3	109.9	109.6
C–H12	109.3	109.3	109.4	109.3	109.3	109.6
C–H13	109.3	109.4	109.6	109.4	109.4	109.4
C–H14	109.3	109.2	109.2	109.5	109.5	109.2
Angles						
C–C–C	112.4	112.8	112.8	112.6	112.8	113.0
C–C–N	108.1	108.0	108.4	115.2	109.2	114.8
C–C–O	112.1	108.9	108.7	105.2	105.0	109.8
C–O–H	103.7	103.7	103.2	107.7	107.5	106.5
C–N–H7	111.3	110.7	110.4	109.1	107.5	108.9
C–N–H8	110.4	109.8	110.4	107.5	109.8	107.3
C–C–H9	109.5	110.5	107.9	109.3	109.0	110.0
C–C–H10	109.5	107.9	110.7	107.8	107.5	108.2
C–C–H11	109.5	108.0	108.8	108.5	107.8	108.8
C–C–H12	109.5	109.6	110.4	109.6	109.8	110.3
C–C–H13	109.5	111.1	111.6	111.1	111.1	111.2
C–C–H14	109.5	109.9	109.5	111.0	110.7	110.3
Dihedral						
C–C–C–N	180.0	186.8	−68.6	181.3	176.1	180.7
N–C–C–O	−55.4	−53.5	54.5	−57.6	−63.1	−54.5
C–C–O–H	28.3	38.7	−41.1	176.3	168.5	−70.3
C–C–N–H7	159.5	163.4	85.4	−61.8	59.2	−67.2
C–C–N–H8	−78.2	−79.3	202.9	52.5	175.0	46.4
O–C–C–H9		180.8	−61.8	179.5	178.0	182.3
O–C–C–H10		62.9	180.3	63.2	61.7	66.3
N–C–C–H11		66.0	170.0	59.7	53.9	58.6
C–C–C–H12		59.2	60.8	59.2	58.7	58.6
C–C–C–H13		−61.5	−60.4	−61.2	−62.0	−60.9
C–C–C–H14		178.1	179.1	178.8	178.2	178.3

Table 2 (*Continued*)

	gG′g		g′Gg′	tG′t	g′G′t	tG′g′
	Ref [6][b]	MP2	MP2	MP2	MP2	MP2
d(OH···N)	213.4	212.4	214.8	371.8	357.8	325.9
d(OH···N)[c]		226.7	229.1	371.0	358.4	329.6
d(NH···O)[e]		327.2	337.0	242.2	237.1	244.2
d(NH···O)[c,e]		330.6	339.2	250.7	245.3	253.4
μ		3.40	3.43	3.12	1.24	1.79
μ[c]		3.14	3.17	2.93	1.08	1.60

[a] Energies relative to the most stable conformer ΔE (kJ mol^{-1}); predicted populations, p (%), at room temperature, were calculated assuming a Boltzmann distribution (the total population of the remaining conformers is predicted as $p = 13.4$ and p=3.4% at the HF and MP2 levels of theory, respectively); bond lengths and distances (pm); angles in (°); total dipole moments, μ (Debye) (1D = 3.33564×10^{-30} C m).

[b] Structural parameters assumed in the microwave study of Marstokk and Møllendal [6].

[c] HF results.

[d] The calculated populations relative to the most stable conformer are shown in parentheses.

[e] Distance between the oxygen atom and the closer amino hydrogen atom.

superior performance of the MP2 method to rationalize these interactions. Indeed, this is also in accordance with previous studies on other molecules where intramolecular hydrogen bonding is important [15,16].

The general agreement between the MP2 calculated structural parameters (including the length of the OH···N hydrogen bond) and those reported for conformer gG′g by Marstokk and Møllendal [6] is very good, except for OH bond length which is predicted 15.9 pm shorter by the calculations. The less good agreement between the calculated and experimental OH bond length has been found for other similar molecules [17] and is essentially related with the fact that, contrary to the calculated equilibrium (R_e) bond lengths, the structural parameters obtained by microwave spectroscopy are vibrationally averaged, and vibrational contributions are relatively more important for the OH bond due to the larger anharmonicity associated with the OH stretching vibration.

The dependence of geometrical parameters (bond lengths and angles) on conformation is also essentially determined by the type and relative importance of the different intramolecular interactions occurring in the various conformers. The MP2 calculated geometries show the usual differences when compared with the HF predictions: bond lengths are systematically longer and angles systematically smaller, a tendency that has been found to improve the general agreement between the theoretical and experimental data [15,16,18–20]. However, calculated changes of those parameters with conformation follow the same pattern as predicted by the two methods, though it is also clear from the structural results that the MP2 wave function accounts much better for the hydrogen bonding. For instance, the hydrogen bonding distances d(OH···N) (in gG′g and g′Gg′) and d(NH···O) (e.g. in tG′t, g′G′t and tG′g′) are considerably shorter at the MP2 level, while the O–C–C–N and C1–C2–O–H dihedral angles become smaller in these conformers having an OH···N hydrogen bond, in order to achieve a more favorable geometry for the establishment of the H-bond.

From the structural data presented in Table 2 it is also possible to conclude that the C–O and C–N bond lengths become shorter (i.e. the bonds become stronger), respectively when the OH···N or NH···O intramolecular hydrogen bond becomes stronger. So, among the five most stable conformers of **1AP**, the C–O bond length attains its minimum value in the most stable conformer (gG′g) and the C–N bond length reaches its minimum value in form tG′t. In addition, as expected, the OH bond length is longer for the conformers having an OH···N bond. On the other hand, the N–H bond length does not appear to be strongly affected by H-bonding, a trend that was also previously observed for **2AP** [5]. Also in accordance with data previously reported for other molecules containing the OH group [5,21], the C1–C2 bond length is predicted to be systematically shorter in those conformers where the hydroxyl group is in a *trans* position (e.g. in forms tG′t and g′G′t; see

Table 2). The valence angles are generally similar in all conformers, the observed differences (which are more relevant for C–C–N, C–C–O and C–O–H) being essentially due to the different type of hydrogen bonding as well as to the different conformation assumed by the hydroxyl group in the various forms.

3.2. Gas phase, solution phase and matrix-isolation infrared spectra

No vibrational spectroscopic data have been previously reported for **1AP**, except for the gas phase [6,22]. In their microwave study of **1AP**, Marstokk and Møllendal [6] were able to identify a few low frequency ($\nu < 260\ cm^{-1}$) vibrations of the most stable gG′g conformer. In addition, they mentioned the observation of some spectral features that could have been due to other conformers, though they could not establish the nature of these forms [6]. As for [22], the gas phase spectrum was not even assigned.

In the infrared spectra of the matrix-isolated compound (Fig. 2) bands due to five different conformers of **1AP** were observed. Table 3 shows the calculated wave numbers and infrared and Raman intensities of the vibrational bands for the most stable conformer of **1AP** predicted by the ab initio calculations (gG′g), together with the potential energy distributions (PEDs).[2] The theoretical data, subjected to the usual scaling procedure, (see Section 2) fit nicely to the experimental observations, as can be noticed by comparing the experimental (argon matrix) with the simulated spectra, also shown in Fig. 2. A detailed assignment of the matrix-isolated (both in argon and krypton) and gas phase spectra is presented in Table 4. Note that in the high temperature gas phase spectrum, where bands are much broader than in the matrix-isolation spectra and extensive overlapping occurs, only bands due to the three most stable conformers (gG′g, g′Gg′ and tG′t) could be unequivocally observed.

Bands belonging to the conformational ground state (g′Gg′) dominate the spectra in the low temperature matrices. The absence of significant contribution of dimers (or higher order aggregates) to the observed spectra was confirmed by comparison with spectra obtained using low matrix/solute ratios (the most intense band of aggregated species should be present around 3260 cm^{-1}). Most of the bands expected for conformers g′Gg′, tG′t, g′G′t and tG′g′ could also be observed both in argon and krypton. As usual, some of the bands appear as multiplets due to matrix-site effects (see Table 4). Since the number of observed conformers is relatively large, matrix-site effects strongly complicate the analysis of the experimental data and the assignments here proposed for the lowest intensity modes of the highest energy conformers must be considered as tentative. Note that as expected considering the greater softness of the krypton matrices the site splitting was found to be less important in this case.

An estimation of the relative populations of the observed conformers in argon and krypton can be obtained by comparing the calculated and observed intensities in the corresponding spectra. Since band intensities were not found to change upon annealing of the matrices up to 30 K, the conformational composition measured by this way must be similar to that of the initial gaseous mixture, which was kept at 298 K. Considering all the possible bands for each conformer, population ratios (gG′g:g′Gg′:tG′t:g′G′t:tG′g′) in argon and krypton were calculated, being 1:0.27:0.23:0.11:0.10 and 1:0.43:0.16:0.15:0.04, respectively. From these results, the following conclusions can be drawn:

- the experimentally observed relative populations of the two most stable conformers estimated using the data obtained from the argon matrix spectrum agree fairly well with the calculated values (MP2: 0.20; HF: 0.14), despite the fact that the calculations seem to underestimate to some extent the population of the most stable conformer;
- the population of the second most stable conformer (g′Gg′, with the largest dipole moment; see Table 2) increases in the Kr matrix. This result seems to indicate that, in this case, partial isomerization of the solute takes place during the deposition process; such phenomenon may be related with a more favorable packing in the Kr matrix for a *gauche* than for a *trans* C3–C2–C1–N conformation, since g′Gg′ is the single observed conformer exhibiting the former arrangement around the C2–C1 bond. Furthermore, this observation also agrees with the

[2] Similar tables for the remaining observed conformers (g′Gg′, tG′t, g′G′t and tG′g′) can be obtained from the corresponding author upon request.

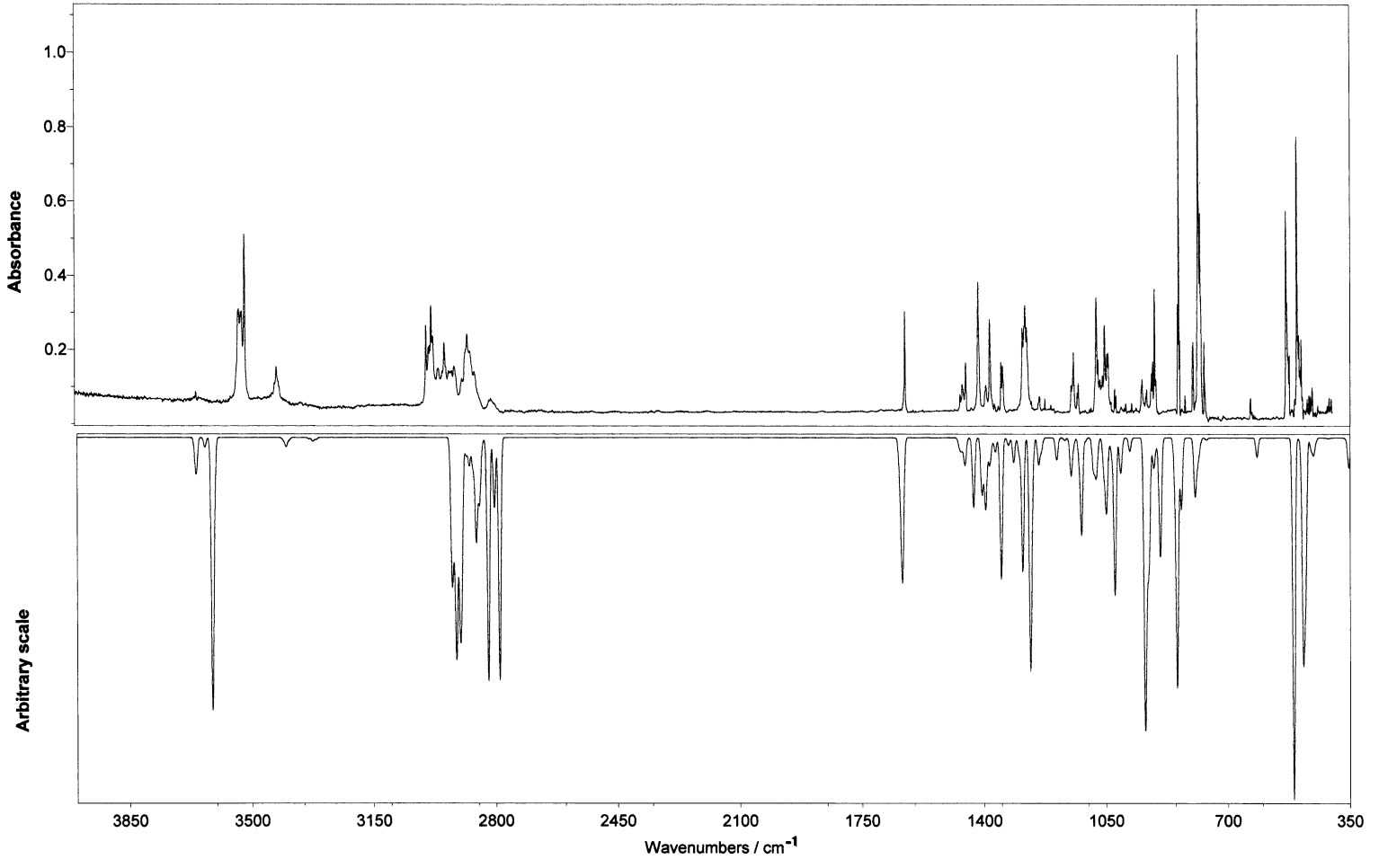

Fig. 2. Low temperature (14 K) infrared spectra of 1-amino-2-propanol isolated in argon (upper) and calculated vibrational spectrum, obtained by Gaussian synthesis (constant half band width assumed) using the results presented in Table 4, and shown in an arbitrary scale (bottom). The experimental spectrum was baseline corrected and the bands due to traces of isolated water monomer were subtracted.

Table 3
HF/6-31G* calculated wave numbers and infrared (IR) and Raman (R) intensities as well as calculated potential energies distributions (PEDs) for form gG′g of 1-amino-2-propanol[a]

ν	I^{IR}	I^{R}	PED[b,c]	Assignment[c]
4059	86.9	52.0	νOH (100)	νOH
3820	2.5	79.4	νNH_2 as. (98)	νNH_2 as.
3734	1.1	99.1	νNH_2 s. (98)	νNH_2 s.
3288	38.6	76.1	νCH_3 as. (94)	νCH_3 as.
3272	67.4	71.4	νCH_3 as.′ (89)	νCH_3 as.′
3254	27.6	33.8	νCH_2 as. (67) + νCH_2 s. (26)	νCH_2 as.
3209	31.3	121.4	νCH_3 s. (96)	νCH_3 s.
3170	67.5	73.8	νCH_2 s. (70) + νCH_2 as. (25)	νCH_2 s.
3134	81.2	93.9	νCH (95)	νCH
1835	39.2	6.9	δNH_2 (78) + ωNH_2 (20)	δNH_2
1650	2.0	16.0	δCH_2 (70) + δCH_3 as.′ (12)	δCH_2
1645	1.8	8.8	δCH_3 as.′ (56) + δCH_2 (22) + δCH_3 as. (11)	δCH_3 as.′
1634	6.6	12.1	δCH_3 as. (51) + δCH_3 as.′ (21)	δCH_3 as.
1607	23.2	0.6	ωCH_2 (17) + γCH (16) + νCC as. (16) + δCH_3 as. (15) + δCOH (14)	γCH
1568	14.2	3.1	δCH_3 s. (48) + ωCH_2 (22)	δCH_3 s.
1536	2.3	7.1	δCH (40) + δCH_3 s. (25)	δCH
1518	45.6	3.7	ωCH_2 (22) + γCH (21) + δCH (15) + γNH_2 (11)	ωCH_2
1448	44.8	7.3	twCH_2 (42) + ωCH_2 (15) + γNH_2 (14) + δCOH (10)	twCH_2
1424	74.7	12.1	δCOH (40) + γCH (32)	δCOH
1340	2.3	2.3	twCH_2 (20) + γNH_2 (18) + γCH_3 (11)	γNH_2
1292	12.1	4.0	νCO (45) + δCH (11)	νCO
1179	22.7	12.8	νCC as. (29) + νCN (29) + δCOH (10)	νCC as.
1151	52.5	1.2	νCN (42) + γCH_3′ (13) + νCC s. (11)	νCN
1134	6.1	0.5	γNH_2 (27) + γCH_3 (25)	γCH_3
1054	89.3	6.3	ωNH_2 (41) + γCH_2 (18)	ωNH_2
1026	8.9	5.9	νCC as. (27) + νCO (23) + γCH_3 (21) + γCH_3′ (15)	γCH_3′
949	80.4	3.9	ωNH_2 (40) + γCH_2 (20)	γCH_2
892	18.0	7.0	νCC s. (35) + ωNH_2 (20)	νCC s.
574	120.9	1.9	τHOCC (39) + δCCO as. (18) + δCCN (14)	δCCO as.
544	68.2	3.4	τHOCC (46) + δCCN (16) + δCCO as. (13)	τHOCC
518	3.6	0.7	δCCO s. (57)	δCCO s.
395	6.8	0.4	δCCO as. (45) + δCCC (25)	δCCC
290	13.4	1.1	τCCNH (61) + τHOCC (12) + δCCC (10)	τCCNH
276	1.6	0.2	δCCN (33) + δCCC (28) + τCCNH (20)	δCCN
248	1.0	0.03	τOCCH (88)	τOCCH
162	2.1	0.1	τOCCN (77) + τHOCC (15)	τOCCN

[a] Wave numbers (ν) in cm^{-1}; IR intensities (I^{IR}) in km mol^{-1}; Raman activities (I^{R}) in $Å^4$ a.m.u.$^{-1}$.
[b] Only PED values larger than 10% are shown in this table.
[c] Abbreviations: ν, stretching; δ, bending; γ, rocking; ω, wagging; τ, torsion; tw, twisting.

well-known tendency for stabilization of more polar species in krypton, due to the higher polarizability of this atom when compared with argon;

- in the case of some low intensity bands ascribed to the less stable observed conformers, extensive overlapping makes the band deconvolution process used to determine intensities extremely difficult. Taking these difficulties into account, the less good agreement between experimental and predicted populations for conformers tG′t, g′G′t and tG′g′ could be anticipated (calculated populations relative to the most stable conformer are predicted to be less than 0.05 both at the MP2 and HF levels of theory). However, since their experimentally observed populations are, in all cases, systematically higher than the predicted values it is also possible that the calculations considerably overestimate the energies of these conformers, which, as discussed

Table 4
Gas phase [22] and low temperature matrix-isolation infrared vibrational spectra, and calculated wave numbers and intensities for the most highly populated conformational states of 1-amino-2-propanol[a]

Assignment[b]	Gas phase[c]		MIS[b]				Calculated	
			Ar		Kr			
	ν	I	ν	I	ν	I	ν	I
νOH III	3653	m	3657	0.7	3659	0.8	3658	4.4
νOH I	3556	m	3537	4.2	3533	15.6	3613	40.4
			3533[d]	9.5	3529[d]	1.8		
			3530[d]	10.3	3524[d]	6.3		
			3527[d]	9.5	3518[d]	17.5		
			3525[d]	4.0	3516[d]	22.2		
			3522[d]	24.5				
νOH II			3514	25.8	3510	34.4	3607	9.3
νNH_2as. II	3446	sh	3428	2.8	3420	2.8	3408	0.4
νNH_2 as. I	3432	w	3423	7.9	3415	10.7	3400	1.2
			3417[d]	10.0	3410[d]	1.6		
νNH_2 s. I	3361	vw	3353	0.7	3345	2.1	3323	0.5
νCH_3as. I	2977	vs	2994	12.7	2983	31.4	2926	17.9
νCH_3as. V			2990	4.2	n. o		2923	1.8
νCH_3as. II			2987	7.4	2979	8.6	2922	5.3
νCH_3as.' III			2984	4.0	2972	12.1	2918	7.1
νCH_3as.' IV			2984	1.7	2972	5.3	2917	3.1
νCH_3as.' I	2977	vs	2980	15.8	2967	12.3	2912	31.3
			2976[d]	7.5				
			2974[d]	8.2				
νCH_3as.' V			2967	3.9	2961	1.1	2904	5.0
νCH_2as. II			2962	2.5	2957	5.8	2903	7.5
νCH_3as.' II			2960	4.2	2953	13.7	2902	8.6
			2958[d]	4.2				
νCH_2as. III			2953	2.6	2946	7.5	2900	4.0
νCH_3as. IV			2951	2.5	n. o		2900	2.8
νCH_3as. III			2948	5.2	2940	3.8	2898	4.5
νCH_2as. I	2946	sh	2942	10.7	2938	3.3	2896	12.8
			2940[d]	5.4	2934[d]	5.8		
νCH_2as. IV			2937	2.8	2931	4.2	2884	2.1
νCH_2as. V			2935	3.8	n. o		2886	0.7
νCH II			2930	6.2	2925	9.3	2876	2.9
νCH V			2925	5.5	2922	2.5	2874	1.6
νCH_2s. III			2921	5.7	2919	5.1	2865	4.6
νCH_3s. I	2927	vs	2915	7.0	2917	7.5	2856	14.5
			2912[d]	5.9	2911[d]	7.5		
νCH IV			2909	5.9	2906	4.1	2854	1.7
					2901[d]	2.7		
νCH_3s. II			2893	6.9	2886	12.7	2848	3.6
νCH_3s. IV			2889	0.6	2890	3.0	2847	2.2
νCH_3s. III			2882	8.5	2876	17.8	2846	2.7
νCH_3s.V			2880	9.8	n. o		2844	2.6
νCH_2s. II			2877	15.2	2872	11.8	2823	7.7
					2870[d]	8.0		
νCH_2s. I	2874	s	2872	13.8	2867	8.2	2821	31.4
			2868[d]	12.8	2863[d]	10.6		
νCH_2s. IV			2864	3.8	2859	15.6	2805	3.0
νCH III			2856	28.9	2849	6.8	2804	8.0
νCH I	2874	w	2810	10.8	2804	29.8	2789	37.7
δNH_2 I	1625	m	1624	[e]	1621	[e]	1633	18.2
δCH_2 IV			1482	0.01	1485	0.2	1474	0.1
δCH_2 I	1470	sh	1467	2.0	1464	4.3	1469	0.9
δCH_2 II			1466	0.6	1468	1.9	1471	0.6
δCH_3as. II			1463	0.8	1458	2.1	1465	0.2
δCH_3as.' I	1470	sh	1460	2.8	1458	8.3	1464	0.8
δCH_3as. III			1458	1.1	n. o		1464	0.3
δCH_3as.' III			1457	2.3	n. o		1459	0.4
δCH_3as.' II			1453	3.9	1448	1.5	1455	0.9
δCH_3as. I	1457	m	1450	3.0	1448	5.1	1454	3.1
			1449[d]	0.6				
δCH_2 III			1435	0.3	1439	0.2	1451	0.01
			1433[d]	0.1				
ωCH_2 IV			1420	0.7	1428	4.2	1428	0.1
γCH I	1439	w	1417	3.5	1414	12.5	1430	10.8
			1415[d]	11.9				
δCH II			1412	8.5	1412	10.3	1406	8.2
γCH III			1410	0.7	1400	3.8	1406	0.4
δCH_3s. I	1392	s	1395	1.1	1393	1.6	1396	6.6
			1392[d]	2.6	1390[d]	4.4		
δCH_3s. IV			1390	1.9	n. o		1395	0.7
δCH_3s. II			1382	6.4	1379	7.4	1393	2.5
δCH_3s. III			1382	3.0	1379	3.5	1393	1.2
ωCH_2 II			1380	6.0	1376	4.6	1384	3.1
δCH_3s. V			1375	1.3	n. o		1380	0.7

Table 4 (*Continued*)

Assignment [b]	Gas phase [c]		MIS [b]				Calculated	
			Ar		Kr			
	ν	I	ν	I	ν	I	ν	I
δCH IV			1372	0.3	n. o		1377	0.4
δCH I	1337	sh	1368	0.6	1366	3.0	1367	1.1
			1366 [d]	0.7	1364 [d]	1.4		
δCH III			1362	0.1	1357	0.2	1368	1.1
twCH$_2$ III			1357	1.2	1354	0.8	1352	0.1
			1355 [d]	0.05				
ωCH$_2$ I	1337	sh	1350	4.8	1347	6.2	1351	21.2
			1345 [d]	8.3				
γCH II			1343	2.7	1343	4.0	1348	1.0
γCH IV			1339	1.9	1338	3.6	1330	1.2
ωCH$_2$ III			1320	2.8	1328	0.8	1315	3.6
					1318 [d]	1.8		
twCH$_2$ II			1317	0.3	1311	2.6	1314	0.3
			1313 [d]	1.5				
twCH$_2$ IV			1301	4.0	1302	1.9	1299	1.6
			1298 [d]	0.2				
γCH V			1294	0.04	1296	2.5	1299	0.9
twCH$_2$ I	1270	m	1288	13.7	1287	7.1	1289	20.8
					1285 [d]	11.1		
δCOH V			1288	0.3	1282	7.5	1271	0.5
δCOH I	1270	m	1284	17.2	1279	10.7	1267	34.7
			1280 [d]	17.1	1275 [d]	11.7		
			1276 [d]	12.0	1271 [d]	14.4		
			1273 [d]	8.0				
δCOH III			1266	0.9	1258	1.4	1261	6.3
			1262 [d]	1.2	1255 [d]	2.1		
δCOH II			1242	3.0	1239	1.7	1243	4.1
			1239 [d]	3.7	1236 [d]	1.6		
γCH$_2$ IV			1224	10.3	1224	0.3	1235	2.0
γNH$_2$ I	1126	m	1209	2.7	1204	2.6	1193	1.1
			1206 [d]	1.2	1202 [d]	0.4		
γNH$_2$ II			1198	0.9	1198	0.1	1191	2.5
			1194 [d]	0.04	1196 [d]	2.2		
νCO IV			1165	0.1	1168	0.2	1168	0.4
			1163 [d]	0.1	1166 [d]	0.6		
γCH$_3$ V			1158	0.4	n. o		1152	0.3
νCO III			1148	4.0	1150	1.7	1143	1.1
					1148 [d]	3.7		
νCO I	1126	m	1146	3.6	1144	7.4	1150	5.6
			1144 [d]	3.4	1141 [d]	1.0		
			1142 [d]	8.8	1139 [d]	6.6		
			1139 [d]	0.6				
νCO V			1136	2.1	1135	3.7	1127	2.7
γCH$_3$ III			1133	0.4	1132	2.0	1120	6.7
			1131 [d]	1.8				

Assignment [b]	Gas phase [c]		MIS [b]				Calculated	
			Ar		Kr			
	ν	I	ν	I	ν	I	ν	I
νCO II			1128	2.3	1130	0.7	1120	8.2
			1126 [d]	0.2	1127 [d]	4.7		
			1124 [d]	0.2	1124 [d]	1.1		
γCH$_3$' IV			1106	0.9	1107	0.3	1109	0.5
νCN III			1097	0.7	1099	1.0	1086	4.8
			1095 [d]	2.3	1098 [d]	0.3		
δCOH IV			1091	1.0	1090	1.9	1079	4.6
νCN V			1080	5.3	1084	0.05	1075	2.6
					1082 [d]	1.2		
νCN II			1076	17.1	1076	9.3	1056	4.7
			1072 [d]	3.9	1072 [d]	4.3		
					1069 [d]	0.8		
γCH$_3$' III			1067	12.0	1066	1.2	1045	1.5
			1065 [d]	0.7	1064 [d]	1.9		
					1062 [d]	2.4		
γNH$_2$ IV			1062	3.6	1058	1.7	1042	0.3
			1060 [d]	1.3	1054 [d]	1.9		
			1058 [d]	3.7				
νCCas. I	1057	s	1056	1.1	1049	10.9	1049	10.5
			1053 [d]	8.1	1046 [d]	6.3		
			1050 [d]	5.7				
γCH$_3$' II			1046	5.1	1039	7.4	1032	1.0
			1044 [d]	3.5	1035 [d]	1.6		
			1042 [d]	5.8				
νCN IV			1034	1.0	1030	0.3	1033	1.3
			1031 [d]	0.1				
νCN I	1057	s	1024	3.9	1027	2.8	1024	24.4
			1021 [d]	0.5	1024 [d]	0.2		
			1020 [d]	2.7	1020 [d]	2.8		
γCH$_3$ I	1057	s	1013	0.5	1015	0.9	1009	2.8
					1012 [d]	0.7		
γNH$_2$ III			1006	1.1	1006	0.7	1006	1.4
γNH$_2$ V			1006	1.5	1002	0.2	1006	1.9
γCH$_3$ II			996	1.9	997	0.7	981	2.1
			993 [d]	1.9	994 [d]	0.7		
					990 [d]	1.7		
γCH$_2$ II			947	3.1	950	2.3	933	11.0
			945 [d]	5.0	944 [d]	3.4		
					941 [d]	2.8		
ωNH$_2$ III			934	2.3	933	2.2	928	11.1
			932 [d]	2.7	930 [d]	2.6		
γCH$_3$ IV			920	2.6	915	5.9	925	3.7
			918 [d]	3.5				
ωNH$_2$ V			915	4.5	911	2.5	925	6.2
νCCas. IV			912	0.2	909	1.4	909	1.1
γCH$_3$' I	926	m	909	12.7	906	7.3	913	4.1

νCCas. II			906	3.6	902	1.3	904	0.7
			903 [d]	0.3				
γCH_3' V			872	1.3	870	0.1	896	5.5
			870 [d]	0.7	865 [d]	0.1		
νCCas. III			842	9.7	842	3.7	893	14.5
ωNH_2 I	834	m	839	24.3	840	8.8	938	41.5
			837 [d]	2.9	837 [d]	7.4		
γCH_2 V			833	0.2	831	0.1	848	0.1
ωNH_2 IV			821	1.0	818	0.01	852	5.5
					813 [d]	0.1		
γCH_2 III			800	4.3	798	2.9	846	0.8
ωNH_2 II			798	5.2	796	5.4	833	11.1
νCCs. IV			795	0.6	790	0.02	794	0.4
γCH_2 I	774	s	787	8.9	782	17.3	845	37.4
			784 [d]	30.4	780 [d]	24.6		
			782 [d]	15.7				
νCCs. I	748	sh	780	7.8	778	2.9	794	8.4
			778 [d]	13.3				
νCCs. III			777	7.4	773	4.9	787	3.5
νCCs. V			773	0.9	768	0.4	781	1.6
νCCs. II			767	3.6	759	0.8	761	0.3
			765 [d]	1.2	757 [d]	0.7		
δCCOs. II	626	w	636	1.9	635	1.3	616	3.0
			634 [d]	3.3	633 [d]	1.3		
δCCOas. I	518	m	533	22.3	532	9.1	511	56.2
δCCOas. V			518	0.1	514	3.9	493	0.3
			517 [d]	0.1				
δCCOas. IV			508	2.7	509	11.5	487	0.8
τHOCC I	478	m	502	26.4	504	5.3	484	31.7
			499 [d]	8.4	501 [d]	42.1		
			496 [d]	7.2				
δCCN III			494	4.4	495	8.2	484	0.2
			492 [d]	3.6				
τHOCC II			489	7.3	489	18.6	477	22.0
			487 [d]	1.4	485 [d]	2.4		
			486 [d]	2.6				
δCCOs. I			472	1.8	459	19.9	461	1.7
			467 [d]	2.5				
			465 [d]	0.4				
			463 [d]	3.6				
			460 [d]	2.9				
			457 [d]	4.8				
δCCOs. IV			448	1.2	440	15.6	449	0.5
δCCOs. III			442	1.4	430	12.1	454	2.4
δCCOas. II			411	0.6	410	2.4	412	0.1
			404 [d]	1.2				

[a] Wavenumbers in cm^{-1}; calculated wavenumbers were scaled by 0.89. MIS experimental intensities are normalised (to 1000) integrated intensities which were measured after deconvolution. Calculated intensities were fitted to Ar experimental normalised integrated intensities (experimental bands assigned to more than one vibration were excluded from the fitting procedure). To obtain *ab initio* intensities (km mol^{-1}) the values presented in the table should be multiplied by 2.1, 8.0, 9.2, 20.2 and 20.6 for those bands ascribed to forms I, II, II, III and V, respectively.

[b] Abbreviations: I, Form **gG'g**; II, Form **g'Gg'**; III, Form **tG't**; IV, Form **g'G't**; V, Form **tG'g'**; ν, stretching; δ, bending; γ, rocking ; ω, wagging; τ, torsion; tw, twisting; n. o., not observed.

[c] Assignment of bands to other conformers than form I are only made when no contribution from this form to the total intensities is expected. Most of the time, bands ascribed to form I also contain minor contributions from other conformers.

[d] Site splitting.

[e] Band overlapped with water band.

before, are characterized by having an NH···O intramolecular hydrogen bond.

In spite of the impossibility of presenting here a detailed discussion of the band assignments, some specific spectral regions were selected for additional comments.

3.2.1. OH stretching region

The analysis of this spectral region is, as usual, complicated by the presence of bands due to isolated monomeric molecules of water. It was, however, possible to assign unequivocally the OH stretching vibration, *v*OH, originating in the three most stable conformers of **1AP** for the matrix-isolated compound. In the gas phase spectrum only two bands are observed, the lower frequency band containing contributions of conformers gG′g (main component) and g′Gg′, and the less intense higher frequency band being ascribable, essentially, to the tG′t form, though it must possess also minor contributions from conformers g′G′t and tG′g′.

Besides being the less populated forms, g′G′t and tG′g′ are predicted by the MP2 calculations to give rise to intrinsically less intense *v*OH vibrations than the most stable forms (the predicted *v*OH intrinsic intensities for g′G′t and tG′g′ are 43.7, 30.2 km mol^{-1}, respectively, and ≈80 km mol^{-1} for the most stable conformers), and it was not possible to assign unequivocally the *v*OH bands due to these forms in the matrix-isolation spectra. The proposed assignments of the *v*OH bands due to the two most populated conformers (gG′g and g′Gg′) is further supported by comparing the relative intensities of the equivalent bands in the argon and krypton spectra, since, as pointed out before, the population of conformer g′Gg′ increases in the krypton matrix. Indeed, the observed intensity ratios of *v*OH(g′Gg′)/*v*OH(gG′g) in argon and krypton are, respectively 0.42 and 0.54 (see Table 4).

In Fig. 3, a correlation between the observed frequency of the *v*OH mode (in argon) and the calculated *d*(OH···N) distance is shown for the most stable conformers of **1AP** as well as for other aminoalcohols previously studied in our laboratory, **2AE**, **2AP** and **3AP**. The Fig. 3 expands the correlation presented in [5], the new data fitting well the linear correlation previously obtained between the MP2 calculated

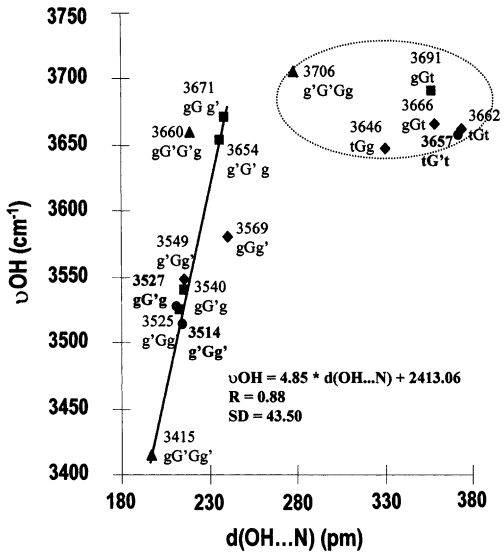

Fig. 3. Plot of experimental frequencies (*v*OH, argon matrix IR spectra) vs. MP2 calculated *d*(OH···N) distances for the most stable conformers of 1-amino-2-propanol (●); 2-amino-1-etanol (◆); 2-amino-1-propanol (■) and 3-amino-1-propanol (▲). The straight line was obtained by fitting the results for the conformers of 2-amino-1-ethanol, 2-amino-1-propanol and 3-amino-1-propanol which present an OH···N intramolecular hydrogen bond [5]; the points relative to 1-amino-2-propanol were added to the plot and shown to match the correlation.

d(OH···N) distance and the observed *v*OH stretching vibration for all conformers exhibiting an OH···N intramolecular hydrogen bond. For these conformers, the shorter the *d*(OH···N) distance — i.e. the stronger the hydrogen bonding — the lower the *v*OH stretching frequency. On the other hand, *v*OH appears at nearly the same frequency in all those conformers which do not have the OH group participating in the OH···N intramolecular hydrogen bonding interaction.

The relative strength of the OH···N intramolecular hydrogen bond in the most stable conformers of the four aminoalcohols studied could be evaluated by the relative values of their *v*OH frequencies. Using the gravity centers of the bands ascribed to the OH stretching mode in each molecule (*v*OH appears in all cases as a multiplet of bands due to matrix-site effects [3–5]), it can be concluded that the strength of the hydrogen bond decreases in the order **3AP** > **1AP** ≈ **2AP** > **2AE** (*v*OH^{gc}: **3AP**, 3415 cm^{-1}; **1AP**, 3527 cm^{-1}; **2AP**: 3525 cm^{-1}; **2AE**: 3549 cm^{-1} — see

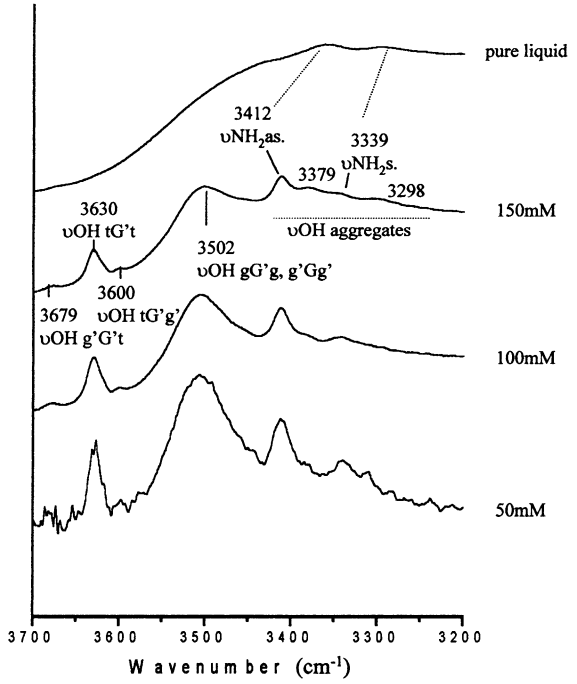

Fig. 4. OH and NH_2 stretching regions of the infrared spectra of 1-amino-2-propanol in CCl_2=CCl_2 solutions.

Table 4 and [3–5]). The gravity centers are calculated as $\nu OH^{gc} = \Sigma(I_i \nu OH_i)/\Sigma I_i$, where the sums extend to all component bands and I_i means the intensity of the component band i.

The assignments of the νOH bands in the matrix-isolated **1AP** spectra are reinforced by the solution studies in tetrachloroethylene. The results obtained in solution are presented in Fig. 4, where νOH bands due to the different conformers and aggregated species can be observed. Contrary to the matrix-isolation spectra, in the solution spectra, it was possible to observe the νOH bands due to the highest energy observed conformers (tG′g′ and g′G′t), since in this case the spectral signal-to-noise ratio is much better, thus enabling detection of the bands originated in the less populated forms. For the lowest concentrations of **1AP**, besides the bands due to the NH_2 symmetric and asymmetric stretching modes, appearing, respectively at 3412 and 3339 cm^{-1}, the spectra show a relatively broad band centered at 3502 cm^{-1} due to the conformers gG′g and g′Gg′, which have a strong OH···N intramolecular hydrogen bond, and three narrower bands, at higher frequencies (3600, 3630 and 3679 cm^{-1}), ascribable, respectively to conformers tG′g′, tG′t and g′G′t, where the OH group is not involved in the OH···N interaction. Note that all bands observed in the solution spectra are red shifted by ca. 30 cm^{-1} with respect to the corresponding bands observed in the matrices, a result that agrees with the relative polarity of the environment. Upon raising the concentration, the bands due to the different monomeric species decrease their intensity, while a very broad band with maxima at 3379, 3298 and 3212 cm^{-1}, ascribable to the νOH vibration of aggregated species containing an OH···N intermolecular hydrogen bond, start to dominate the spectra.

3.2.2. NH_2 wagging vibration

Accordingly to the calculations, the NH_2 wagging vibration should give rise to an intense infrared band. Based in its intensity, in the most stable conformer this mode can be unequivocally assigned to the doublet at 839 and 837 cm^{-1} (in argon). However, the calculations predict that this mode should occur at a higher frequency (calculated value: 938 cm^{-1}), the relative error in the theoretical value being clearly larger for this than for all other vibrations. A similar situation happens for the ωNH_2 vibration of conformer g′Gg′, which is also a conformer having a strong OH···N intramolecular hydrogen bond. On the other hand, the agreement between the calculated and experimental frequencies for this mode in the remaining observed conformers is much better, despite a general overestimation of the calculated frequencies being noticed. (see Table 4). It is well known that ab initio calculations carried out at the level of theory used here cannot account for some subtle effects associated with hydrogen bonding [15,23]. So, the involvement of the nitrogen atom in the OH···N intramolecular hydrogen bond, where it acts exclusively as hydrogen bond acceptor, seems to contribute, at least in part, to the red shift of the frequency of the ωNH_2. A possible explanation for this is to consider that, when the amino group is involved in a strong OH···N intramolecular hydrogen bond, the nitrogen lone electron pair becomes more concentrated along the direction of this bond, and this electronic migration opens up more space for the wagging vibration of the amino hydrogen atoms to occur, thus reducing the force constant associated with this coordinate and, consequently, red shifting its frequency. It is worth mentioning that

a similar effect was also previously observed for **2AP** [5].

3.2.3. Low frequency vibrations

The spectral region below 400 cm^{-1} was not experimentally investigated in this study, but the calculations provide estimations for the frequencies of the vibrations that should give rise to bands in this region. As mentioned above, some of the low frequency modes of the most stable conformer of **1AP** were reported by Marstokk and Møllendal [6], who also proposed their assignments. The results of the ab initio calculations presented now confirm the assignments made by those authors. Thus, the frequencies of the τOCCN, τCCCH and τCCNH modes obtained from the microwave spectra of **1AP** (139 ± 15, 221 and 255 ± 25 cm^{-1} [6]), may be compared with the corresponding theoretical (scaled) frequencies: 144, 221 and 258 cm^{-1}.

3.3. Temperature variation infrared studies (annealing of the matrices)

The results of Barnes [24,25] indicate that energy barrier heights higher than 10–12 kJ mol^{-1} are needed in order to avoid establishment of a conformational thermal equilibrium for a substance in a matrix annealed to ca. 30 K. Thus, both argon and krypton matrices were annealed to about this temperature, in order to search for any substantial reorganization of relative band intensities. Within the range of temperatures covered, no evidence was found of conformer isomerization, indicating that energy barriers separating the different observed conformers are higher than 10–12 kJ mol^{-1}, in agreement with previous data on **2AE** [14] and **2AP** [5].

3.4. Liquid phase infrared and Raman spectra

Fig. 5 shows the infrared and Raman spectra of liquid **1AP**. The proposed assignments are presented in Table 5.

Most of the bands of the spectra of the aggregates can be fairly well assigned taking as reference the calculated spectra of the monomeric form tG′t, which indicates that the monomeric units within the aggregates assume a conformation similar to this form. The intramolecular NH···O hydrogen bond exhibited by this conformer (the lowest energy form with an intramolecular NH···O hydrogen bond in isolated **1AP**) makes the hydroxyl group more acidic and the amino group more basic, and then activates both OH and NH_2 groups in order to establish the OH···N intermolecular hydrogen bond, the dominant intermolecular interaction present in the aggregated species. The importance of this intermolecular hydrogen bond in liquid **1AP** is also reflected in the frequencies of the bands assigned to *v*O–H, which strongly decrease when compared with those of the free monomeric species, and to τHOCC, which increases when the OH group is involved in the intermolecular H-bonding [26] (see also Tables 4 and 5). These results are in agreement with the conclusions of our previous studies on **2AE**, **2AP** and **3AP**, where conformations structurally similar to form tG′t of **1AP** were also found to be the preferred conformations assumed by the monomeric units within the aggregates, in the liquid phase [3–5].

As for **2AE** and **2AP** [3,5], and contrary to what was found for **3AP** [4], temperature variation studies carried out on the pure liquid show that there are no detectable amounts of free monomeric molecules in the pure liquid **1AP**. The different behavior of **3AP**, when compared with the remaining aminoalcohols, has been correlated with the larger conformational flexibility in **3AP**, which leads to a more favorable OH···N intramolecular hydrogen bonding interaction geometry [4,5,27]. Indeed, in general the most fundamental factors leading to energetically more favorable intermolecular hydrogen bonding relatively to intramolecular hydrogen bonding are geometrical requirements, which can be easier attained in the case of the first type of interaction. The results now obtained for **1AP** reinforce the interpretation previously made on this basis [3–5] since **1AP** has a conformational flexibility which is similar to those of **2AP** and **2AE**, but smaller than that of **3AP** (i.e. the energetic balance associated with intra- versus intermolecular hydrogen bonding is relatively more favorable to the first type of interaction only in the more flexible **3AP** than in the remaining molecules).

In the liquid phase spectra of **1AP**, there is also some evidence pointing to the presence in the liquid of a minor amount of monomeric units assuming a completely different conformation within the aggregates. This gives rise, for instance, to the low intensity

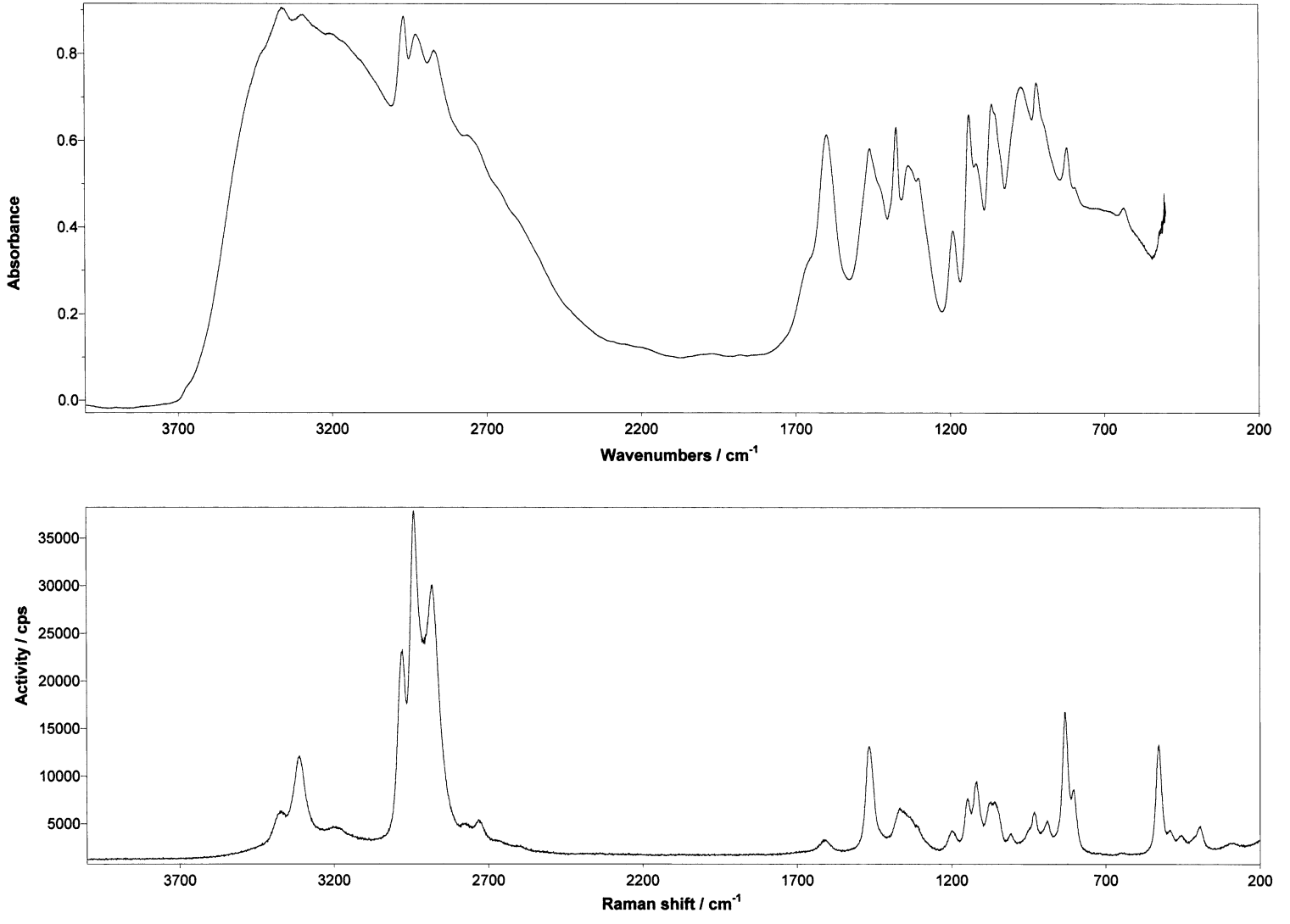

Fig. 5. Room temperature liquid phase infrared (upper) and Raman (bottom) spectra of 1-amino-2-propanol. Raman activities were presented in counts-per-second (cps).

Table 5
Comparison of the infrared (IR) and Raman (R) spectra of pure liquid with the calculated spectra of form tG′t (see text)[a]

Infrared		Raman		Calculated			Assignment[b]
ν	I^{ir}	ν	I^{R}	ν	I^{ir}	I^{R}	
3359	vs	3377	23.1	3393	2.9	38.5	νNH_2as.
3295	vs	3312	70.1	3314	2.0	62.0	νNH_2s.
3202	vs	3196	61.7	3658[c]	40.1	64.5	νOH
2967	vs	2982	51.3	2918	65.2	59.2	νCH_3as.
				2900	36.8	34.3	νCH_2as.
2926	vs	2939	207.8	2898	41.6	44.1	νCH_3as.
				2865	42.5	85.5	νCH_2s.
				2846	24.4	70.9	νCH_3s.
2867	vs	2881	192.5	2804	73.1	70.1	νCH
1598	s	1611	7.2	1640	31.8	4.6	δNH_2
1458	s	1465	45.4	1464	2.4	9.2	δCH_3as.
				1459	3.8	11.8	δCH_3as.
1422	sh			1451	0.1	3.6	δCH_2
				1406	3.7	5.6	γCH
1374	s	1368	50.7	1393	11.4	2.6	δCH_3s.
				1368	9.9	4.6	δCH
1335	m	1336	22.7	1352	1.2	8.3	$twCH_2$
1301	m	1307	2.9	1315	33.0	2.3	ωCH_2
1190	m	1196	9.1	1261	57.6	4.0	δCOH
1137	s	1149	13.6	1143	10.1	3.3	νCO
1115	m	1117	27.3	1120	61.8	1.7	γCH_3
1064	s	1078	19.1	1086	43.9	4.0	νCN
1053	s	1055	14.0	1045	13.6	1.2	γCH_3
1035	sh	1008	7.2	1006	12.7	5.4	γNH_2
968	s	950	13.2	928	101.8	3.3	ωNH_2
919	s	931	16.3	893	133.2	2.3	νCCas.
894	sh	890	12.7	846	7.1	1.5	γCH_2
821	m	831	47.1	787	32.0	7.2	νCCs.
		528	32.9	280[c]	71.9	3.6	τHOCC
		490	13.1	484	2.2	3.6	δCCN
		455	4.7	454	22.1	0.3	δCCOs.
		394	8.6	354	9.5	0.7	δCCOas.
		281	25.5	288	116.0	0.8	τCCNH
				236	10.1	0.3	δCCC
				226	1.4	0.03	τOCCH
				127	5.6	0.08	τOCCN

[a] Wavenumbers, ν, in cm^{-1}; calculated wavenumbers were scaled by 0.89. Infrared experimental intensities (I) presented as qualitative relative intensities; infrared *ab initio* intensities in km mol^{-1}. Raman experimental intensities are normalised (to 1000) integrated intensities which were measured after deconvolution; Raman calculated intensities were fitted to Raman experimental normalised integrated intensities (experimental bands assigned to more than one vibration were excluded from the fitting procedure). To obtain Raman *ab initio* intensities ($Å^4$ $a.m.u.^{-1}$) the values presented in the table should be multiplied by 1.28.
[b] Abbreviations: ν, stretching; δ, bending; γ, rocking ; ω, wagging; τ, torsion; tw, twisting.
[c] As usually observed [26], when the OH group participates in H-bonding, the wavenumber of νOH decreases while that of τHOCC increases relatively to the isolated molecule situation.

bands at 1665 cm^{-1} (IR), 795 cm^{-1} (IR)/804 cm^{-1} (R), 637 cm^{-1} (IR)/648 cm^{-1} (R) and 416 cm^{-1} (R). These frequencies are similar to those of the δNH_2, ωNH_2, δCCO s. and δCCO as. vibrations of the conformers having a *gauche* C–C–C–N conformation (e.g. g′Gg′: 1638, 798, 636 and 441 cm^{-1}; Table 4), while in the conformers where this conformation is *trans*, these two modes give rise to bands that occur at considerably different frequencies (see Table 4). Thus, the results seem to indicate that the second most stable conformation assumed by the monomeric units within the aggregates in the liquid phase is in all possibility one having a *gauche* C–C–C–O conformation. Though the following assignment should still be seen as tentative, we propose that, since such structure should have its hydroxyl group participating in an intermolecular hydrogen bonding (which excludes form g′Gg′), and considering the relative structures of the different conformers presented in Table 1, the best candidate is a structure close to form gGt.

Acknowledgements

The authors wish to thank Dr. João Cecílio for his technical help. This work was funded by the PRAXIS XXI (P/QUI/10137/1998) research programme, also partially funded by FEDER. C. Cacela acknowledges a PhD grant (GGPXXI/BD/3873/96) from Fundação para a Ciência e Tecnologia, Lisbon.

References

[1] R.L. Sutton, Chem. Br. 27 (1991) 432.
[2] P.M. Mehl, Thermochim. Acta 226 (1993) 325.
[3] C.F.C.P. Silva, M.L.T.S. Duarte, R. Fausto, J. Mol. Struct. 482/483 (1999) 591.
[4] C. Cacela, M.L. Duarte, R. Fausto, Spectrochim. Acta 56A (2000) 1051.
[5] R. Fausto, C. Cacela, M.L. Duarte, J. Mol. Struct. 550/551 (2000) 365.
[6] K.-M. Marstokk, H. Møllendal, J. Mol. Struct. 35 (1976) 57.
[7] Microcal Origin (Version 4.0), copyright © 1991–1995 Microcal Software, Inc. Northampton, MA 01060, USA.
[8] K.K. Irikura, SYNSPEC, Physical and Chemical Properties Division, National Institute of Standards and Technology, Gaithersburg, MD 20899, USA, 1995.
[9] W.J. Hehre, R. Ditchfield, J.A. Pople, J. Chem. Phys. 56 (1972) 2257.
[10] M.J. Frisch, G.W. Trucks, H.B. Schlegel, P.M.W. Gill, B.G. Johnson, M.W. Wong, J.B. Foresman, M.A. Robb, M. Head-Gordon, E.S. Replogle, R. Gomperts, J.L. Andres, K. Raghavachari, J.S. Binkley, C. Gonzalez, R.L. Martin, D.J. Defrees, J. Baker, J.J.P. Stewart, J.A. Pople, GAUSSIAN92/DFT (Revision G.2), Gaussian Inc., Pittsburg, PA, 1993.
[11] H.B. Schlegel, PhD Thesis, Queen's University, Kingston, Ont., Canada, 1975.
[12] D.J. Defrees, A.D. McLean, J. Chem. Phys. 82 (1985) 333.

[13] M.D.G. Faria, R. Fausto, TRANSFORMER, BUILD-G and VIBRAT (Version 1.0), Departamento de Química, Universidade de Coimbra, Portugal, 1990.
[14] M. Räsänen, A. Aspiala, L. Homanen, J. Murto, J. Mol. Struct. 96 (1982) 81.
[15] A. Kulbida, M.N. Ramos, M. Räsänen, J. Nieminen, O. Schrems, R. Fausto, J. Chem. Soc., Faraday Trans. 91 (1995) 1571.
[16] S.G. Stepanian, I.D. Reva, E.D. Radchenko, M.T.S. Rosado, M.L.T.S. Duarte, R. Fausto, L. Adamowicz, J. Phys. Chem. A 102 (1998) 1041.
[17] E.M.S. Maçôas, MSc Thesis, Department of Chemistry, University of Coimbra, Portugal, 2001, and references therein.
[18] R. Ditchfield, K. Seidman, Chem. Phys. Lett. 54 (1978) 57.
[19] D.J. Defrees, B.A. Levi, S.K. Pollack, W.J. Hehre, J.S. Binkley, J.A. Pople, J. Am. Chem. Soc. 101 (1979) 4085.
[20] F.P.S.C. Gil, R. Fausto, A.M. Amorim da Costa, J.J.C. Teixeira-Dias, J. Chem. Soc., Faraday Trans. 90 (1994) 689.
[21] J.J.C. Teixeira-Dias, R. Fausto, J. Mol. Struct. 144 (1986) 199.
[22] EPA Vapor Phase Library (CAS 156-87-6), Galactic Industries Corp., 395 Main ST. Salem, NH 03079, USA, 1994.
[23] M.T. Rosado, M.L.T.S. Duarte, R. Fausto, Phosph. Sulf. Silic. 16 (1996) 153.
[24] A.J. Barnes, in: A.J. Barnes, W.J. Orville-Thomas, A. Müller, R. Gaufrès (Eds.), Matrix Isolation Spectroscopy, D. Reidel, Dordrecht, 1981, p.531.
[25] A.J. Barnes, G.C. White, in: Proceedings of the 12th European Congress on Molecular Spectroscopy, Elsevier, Amsterdam, 1976, p. 373.
[26] R. Fausto, J. Mol. Struct. 377 (1996) 181.
[27] A.-M. Kelterer, M. Flock, M. Ramek, J. Mol. Struct. (Theochem.) 276 (1992) 61.